


Involvement of Hyperpolarization-Activated Cyclic Nucleotide-Gated Channel 3 in Oxytocin Neuronal Activity in Lactating Rats With Pup Deprivation

Dongyang Li¹, Haitao Liu¹, Xiaoyu Liu¹, Hongyang Wang¹,
Tong Li¹, Xiaoran Wang¹, Shuwei Jia¹, Ping Wang², and
Yu-Feng Wang¹ 

ASN Neuro
Volume 12: 1–16
© The Author(s) 2020
Article reuse guidelines:
sagepub.com/journals-permissions
DOI: 10.1177/1759091420944658
journals.sagepub.com/home/asn


Abstract

Oxytocin, a hypothalamic neuropeptide essential for breastfeeding, is mainly produced in oxytocin neurons in the supraoptic nucleus (SON) and paraventricular nucleus. However, mechanisms underlying oxytocin secretion, specifically the involvement of hyperpolarization-activated cyclic nucleotide-gated channel 3 (HCN3) in oxytocin neuronal activity, remain unclear. Using a rat model of intermittent and continuous pup deprivation (PD) at the middle stage of lactation, we analyzed the contribution of HCN3 in oxytocin receptor (OTR)-associated signaling cascade to oxytocin neuronal activity in the SON. PD caused maternal depression, anxiety, milk shortage, involution of the mammary glands, and delays in uterine recovery, particularly in continuous PD. PD increased hypothalamic but not plasma oxytocin levels in enzyme-linked immunosorbent assay. In the SON, PD increased c-Fos expression but reduced expressions of cyclooxygenase-2 and HCN3 in Western blots and/or immunohistochemistry. Moreover, PD significantly increased the molecular association of OTR with HCN3 in coimmunoprecipitation. In brain slices, inhibition of HCN3 activity with DK-AH269 blocked prostaglandin E₂-evoked increase in the firing activity and burst discharge in oxytocin neurons in patch-clamp recordings. In addition, oxytocin-evoked increase in the molecular association between OTR and HCN3 in brain slices of the SON was blocked by pretreatment with indomethacin, an inhibitor of cyclooxygenase-2. These results indicate that normal activity of oxytocin neurons is under the regulation of an oxytocin receptor–cyclooxygenase-2–HCN3 pathway and that PD disrupts maternal behavior through increasing intranuclear oxytocin secretion in the SON but likely reducing bolus oxytocin release into the blood through inhibition of HCN3 activity.

Keywords

breastfeeding, HCN3 channel, maternal behavior, supraoptic nucleus

Received May 1, 2020; Revised June 4, 2020; Accepted for publication June 7, 2020

Oxytocin is a neuropeptide mainly produced in the supraoptic nucleus (SON) and paraventricular nucleus. Oxytocin causes contraction of myometrial cells to promote uterine recovery and of myoepithelial cells to cause milk ejections (Gimpl and Fahrenholz, 2001). Oxytocin is also critical for maternal behavior. In oxytocin knockout mice, maternal behavior is incomplete (Caldwell et al., 2017). In humans, oxytocin also enhances positive social memory (Campbell, 2010). Thus, oxytocin is important for both breastfeeding and maternal behavior.

In normal lactation, a pulsatile pattern of oxytocin neuronal activity is more important than tonic neuronal

activity for the milk-ejection reflex (Wakerley et al., 1994; Hatton and Wang, 2008) and social desirability (Nissen

¹Department of Physiology, School of Basic Medical Sciences, Harbin Medical University

²Department of Genetics, School of Basic Medical Sciences, Harbin Medical University

Corresponding Author:

Yu-Feng Wang, Department of Physiology, School of Basic Medical Sciences, Harbin Medical University, 157 Baojian Road, Nangang, Harbin 150081, China.

Email: yufengwang@ems.hrbmu.edu.cn



et al., 1998). The pulsatility of oxytocin secretion relies on the maturation of hypothalamic machinery for the milk-ejection reflex around parturition and on the ability of oxytocin neurons to discharge burst of action potentials in synchrony during lactation (Russell et al., 2001; Hatton and Wang, 2008; Hou et al., 2016). The burst synchrony depends on coordinative activities of neurochemical environment, particularly increase in somatodendritic oxytocin secretion in the hypothalamus (Neumann et al., 1993), oxytocin receptor (OTR)-associated signaling events (Hatton and Wang, 2008), intercellular junctional coupling (Wang et al., 2019), and astrocytic plasticity (Wang and Hatton, 2009b). Among these factors, OTR has been identified on oxytocin neurons and their adjacent astrocytes in the SON (Wang and Hatton, 2006). The activation of OTR leads to activation of Gq protein and mobilization of $\beta\gamma$ subunits, which induce cyclooxygenase-2 expression and phosphorylation of extracellular signal-regulated protein kinase 1/2 (pERK1/2; Hatton and Wang, 2008). In these signaling events, prostaglandin E₂ (PGE₂), a major product of cyclooxygenase-2, is likely the mediator of OTR-associated burst firing. This is because PGE₂ can evoke more than 70% of oxytocin neurons to discharge burst firing in brain slices, while oxytocin can evoke the burst in less than 30% of oxytocin neurons (Wang et al., 2016). The burst firing in oxytocin neurons has been linked to a rebound firing feature of oxytocin neurons (Armstrong et al., 2019). Among several known ion channels on oxytocin neurons, hyperpolarization-activated cyclic nucleotide-gated channels (HCNs) have the feature of rebound excitation and burst-evoking ability (Qiu et al., 2005; Ying et al., 2011). Among 4 subtypes of HCNs, HCN3 is 5- to 11-fold higher than other subtypes in oxytocin neurons in the SON and blocking HCNs significantly decreases oxytocin neuronal activity (Pires da Silva et al., 2016). Thus, it is very likely that HCN3 is involved in the generation of burst firing. However, it remains a question whether HCN3 activity is regulated by OTR-associated signaling events in the firing activity of oxytocin neurons.

To resolve this question, using a rat model of pup deprivation (PD; Wang and Hatton, 2009a; Liu et al., 2016), we observed effects of different extents of PD on maternal behavior and lactation as well as the association between HCN3 activity and OTR-associated signaling events. The results proved that interactions of OTR signals with HCN3 are essential in burst firing, which can be disrupted by PD.

Materials and Methods

Sprague-Dawley virgin female rats (7–8 weeks old/150–200 g) and male rats (6–7 weeks old/120–150 g for *in vitro* study; 30–40 weeks old/300–400 g for breeding) were

housed in a 12:12 hr light–dark cycle with free access to food and water. All the procedures were conducted in accordance with the National Institutes of Health Guidelines for the Care and Use of Animals and approved by the Animal Care and Use Committees of Harbin Medical University.

Preparation of PD Model

In preparation of lactating rats, one breeder male and two virgin female rats were housed in the same cage until the presence of a vaginal plug. Pregnant female rats were housed individually until parturition. The number of pups was adjusted to 10 per litter. Lactating rats were randomly divided into control, intermittent (IPD), and continuous (CPD) PD groups at Postpartum Day 8 (i.e., PD Day 1). The IPD was established by separating pups from the dams for 20 hr/day (reunion during 4–8 p.m.) starting from 8 a.m. on PD Day 1. The pups were nursed by foster dams during the separation. The CPD group was made by deprivation of pups without reunion except the period of observations in the morning of Postpartum Day 12 (i.e., PD Day 5). Control dams and pups received the same handling procedure as the PD dams except the separation.

Observation of Maternal Behavior

Maternal behavior includes the activities that realize the mother to the pup care. It includes nest building, pup retrieving, licking specially pups' anogenital regions, intruder aggression, nursing posture over pups, and suckling in rat dams. In this study, we analyzed the maternal behavior and lactation performance as previously described (Liu et al., 2019). Litter's body weight gain (LBWG) was evaluated on PD Days 1 to 4 in control and IPD dams, and pup's urine was squeezed out before dam–pup reunion. LBWG was calculated by weighing the pups' weight before and after the reunion. On PD Day 5, lactation performance was observed in all groups during 1 hr or 4 hr suckling except otherwise described. At the first 30 min, several key maternal behaviors were observed including the number and latency of pup retrieval (the first pup), suckling, and anogenital licking. The observation was also videotaped for later analyses. The brain, blood, mammary glands, and uteri of the dams were sampled at 30 min after the final observation in the morning of PD Day 5.

Tissue Preparation

For *in vitro* study, brain slices containing the SON were prepared from male rats as previously described (Wang et al., 2016). In brief, rats were decapitated with a guillotine; brains were quickly removed and placed in ice-cold oxygenated slicing solution. The slicing solution

contained (in mmol/L) 213 sucrose, 2.5 KCl, 5 MgCl₂, 3 CaCl₂, 1.25 NaH₂PO₄, 26 NaHCO₃, and 10 glucose, 305 mOsm/kg, pH 7.4. Coronal hypothalamic slices containing the SON were cut at 300- μ m thick with a vibratome (World Precision Instruments, Sarasota, FL, USA). The slices were then transferred into an artificial cerebrospinal fluid and incubated at 37°C for 30 min before maintenance at room temperature. The artificial cerebrospinal fluid contained (in mmol/L) 126 NaCl, 3 KCl, 2 MgCl₂ and 2 CaCl₂, 1.3 NaH₂PO₄, 20 NaHCO₃, 10 glucose, 305 mOsm/kg, pH 7.4 maintained with a gas mixture of 5% CO₂ and 95% O₂. The slices were divided into the following groups: control, oxytocin (10 pmol/L, O6379, Sigma-Aldrich, Shanghai, China), and indomethacin (5 μ mol/L, inhibitor of cyclooxygenase-2, I7378, Sigma-Aldrich, Shanghai, China) + oxytocin. Oxytocin was applied for 10, min and the blockers were applied at 5 min before oxytocin application. After treatments, the SON was punched out in ice-cold artificial cerebrospinal fluid and then used for protein analyses.

Hematoxylin and Eosin Staining

For identifying the histological features of the mammary glands and uteri, after observations, they were dissected and fixed in 4% paraformaldehyde and then used for conventional hematoxylin and eosin staining. After dehydration with graded alcohol, xylene was used to hyalinize the tissues before paraffin imbedding. Wax blocks were sectioned into 5- μ m thick sections by paraffin slicer (Leica, Wetzlar, Germany). The sections were then deparaffinized, rehydrated, stained with hematoxylin solution (DH0006, Leagene, Beijing, China), treated with 1% hydrochloric acid alcohol, and washed in distilled water. The sections were then stained with eosin solution for 30 s and followed by dehydration with graded alcohol solutions and cleared in xylene. The sections were mounted on glass slides, examined using a digital microscope (PeciPoint M8-Digital Microscopes & Scanner, Freising, Germany), and photographed. The staining was analyzed with PeciPoint software and expressed as relative lengths and areas.

Immunohistochemistry

To identify spatial distribution and relative intensity of HCN3 in oxytocin neurons, the SON was dissected from half of the hypothalamic blocks, sharing with those used for protein analysis. The brain with intact optic chiasm was fixed with 4% paraformaldehyde for 24 hr and then cut into 75- μ m thick sections that contain the SON. The sections were treated with 0.3% Triton X-100 for 1 hr to permeabilize the plasma membrane and then with 5% bovine serum albumin for 1 hr to block nonspecific binding site for the antibodies. After incubation with the

primary antibodies against HCN3 (sc-46354, goat antibody, 1:500, Santa Cruz Biotechnology, Shanghai, China, RRID: AB_2120021), and oxytocin-neurophysin (MAbN844, mouse Ab, 1:3000, Merck Millipore, RRID: AB_2315026, Shanghai, China) at 4°C overnight, species-matched secondary antibodies (ab150135, preadsorbed Alexa Fluor 647-labeled donkey anti-goat IgG H&L, RRID: AB_2687955; ab150062, preadsorbed Alexa Fluor 555-labeled donkey anti-rabbit IgG H&L, RRID: AB_2801638; and ab150109, preadsorbed Alexa Fluor 488-labeled donkey anti-mouse IgG H&L, 1:600, Abcam, RRID: AB_2571721, Shanghai, China) were applied for 2 hr to label the corresponding primary antibodies. Otherwise, Alexa Fluor 647 Streptavidin (35104ES60, Yeasen, Shanghai, China) was used for identify the neurons in patch clamp. Last, Hoechst (CAS# 28718-90-3, Shanghai, China; 0.5 mg/ml, 30 min) was used to label nuclei. Sections were examined with a fluorescence microscope (Eclipse FN1, Nikon, Tokyo, Japan) through a charge-coupled device camera (DS Ri2, Nikon, Tokyo, Japan) or a confocal microscope (Eclipse Ti, Nikon, Tokyo, Japan). To reduce the variability of results from different loci, sections of equivalent location in the mammary glands from different groups were used for comparisons. The specificity of the antibodies was verified by applying no-primary and no-secondary antibody control staining.

Western Blots

The methods of extracting proteins and running Western blots were the same as previously described (Wang et al., 2013). In brief, tissues were homogenized to release proteins in a radioimmunoprecipitation assay lysis buffer (20115ES60, Yeasen, Shanghai, China) with a tissue lyser. Protein concentration was measured at 562 wavelength using bicinchoninic acid assay agent (20201ES76, Yeasen, Shanghai, China). After denaturation, 35 μ g of proteins were loaded in each lane and separated on 10%, 15%, or gradient sodium dodecyl sulfate-polyacrylamide gel electrophoresis gels according to the size of proteins analyzed and then transferred onto polyvinylidenedifluoride membrane. The protein membrane was blocked with 5% bovine serum albumin in TBS containing 0.1% Tween 20 for 2 hr at room temperature (21°C–23°C) and then incubated overnight at 4°C with antibodies against extracellular signal-regulated protein kinase 1/2 (ERK1/2, sc-135900, mouse antibody, 1:500, RRID: AB_2141283, Shanghai, China), pERK1/2 (OM125780, rabbit antibody, 1:500, Omnimabs, Shanghai, China), c-Fos (OM205693, rabbit antibody, 1:500, Omnimabs, Shanghai, China), OTR (OM160599, rabbit antibody, Omnimabs, Shanghai, China), cyclooxygenase-2 (sc-376861, mouse antibody, 1:500, RRID: AB_2722522, Shanghai, China), HCN3 (sc-46354, goat antibody,

1:500, Santa Cruz Biotechnology, Shanghai, China), β -tubulin (30302ES60, rabbit antibody, 1:2000, Yeasen, Shanghai, China), or glyceraldehyde 3-phosphate dehydrogenase (OM254102, rabbit antibody, 1:2000, Omnimabs, Shanghai, China). After washing, the protein membranes were further incubated with corresponding HRP-conjugated secondary antibodies (703-035-003, Peroxidase AffiniPure donkey anti-goat IgG H&L, RRID: AB_2340385; 111-035-003, Peroxidase AffiniPure goat anti-rabbit IgG H&L, RRID: AB_2313567; 115-035-003, Peroxidase AffiniPure goat anti-mouse IgG H&L, RRID: AB_10015289, Jackson Lab, Shanghai, China). Protein bands were visualized with an automated chemiluminescence imaging analysis system (Tanon 5200, Shanghai, China). The specificity of primary antibodies was verified by immunoneutralization before the study.

Coimmunoprecipitation

Two methods were used for coimmunoprecipitation experiments. For assaying molecular association between molecules in lactation rats, the protocol was the same as previously described (Wang et al., 2019). Briefly, total tissue lysates of the SON were precleared with protein A/G agarose beads (sc-2003, RRID: AB_10201400) to reduce nonspecific binding. To form immunocomplex, immunoprecipitating antibody against OTR (1.5 μ g, rabbit antibody, OM160599, Shanghai, China) was added to 500 μ l of protein lysis buffer containing 600 μ g of protein lysates, and the reaction was incubated overnight at 4°C on a rotator. The immunocomplex was captured by 50 μ l slurry of protein A/G agarose beads with gently rocking for 2 hr at 4°C. The beads were then collected by a pulse centrifugation. After removing the supernatant and washing, the beads were resuspended in 2 \times sample buffer (25 μ l, P0015B, Beyotime, Shanghai, China), heated for 10 min at 100°C to dissociate and denature the immunocomplex and then spun down to collect supernatant for running Western blots as described earlier.

To pull down target proteins in male rats, biological nanosurface technology was adopted in coimmunoprecipitation. That is, after precleaning with regular agarose beads and forming immunocomplex (350 μ g protein lysate plus 1.0 μ g immunoprecipitating antibody), the antigen-antibody complex was captured with 30 μ l of protein A/G magnetic beads (B23202, RRID: AB_1651895, Bimake, Houston, TX, USA) on an orbital shaker for 2 hr at 4°C. Then, protein-bead complex was separated from nonbinding proteins in the supernatant with a magnetic separator and then kept in 4°C following rinsing the beads. The supernatant was resuspended and incubated with 10 μ l magnetic beads at room temperature for 30 min to capture the remaining immunocomplex. All

the beads were pooled together, denatured, and run for Western blots as described earlier. The proteins to be detected were HCN3 (ab84818, mouse antibody, 1:1000, RRID: AB_1861081, Abcam, Cambridge, UK) and OTR as detailed in the result.

Enzyme-Linked Immunosorbent Assay of Oxytocin Levels

To assay blood oxytocin levels, trunk blood samples were collected after decapitation, with 30-min interval from the last observation. Then, plasma was collected through a centrifugation at 3,000 rpm for 15 min at 4°C and stored at -80°C until the assay. Assaying plasma oxytocin level was performed in accordance with the instructions of assay manual provided by the company (CEB052Ge, Cloud-Clone Corp., Wuhan, China). In brief, the standard was prepared in a series of dilution (3,000, 1,000, 333.33, 111.11, 37.04, 12.35, and 0 pg/ml). Samples were thawed and warmed to room temperature for assays in duplicates. Standard or sample solutions (50 μ l) were respectively added to the assigned wells; 50 μ l of detection reagent A was added to all wells. The reaction was incubated for 1 hr at 37°C and washed with 350 μ l of wash solution for three times. Then, 100 μ l of detection reagent B was added to each well, which was kept for 30 min at 37°C. After rinsing and drying, 90 μ l of substrate solution was added and kept for 15 min for coloration before the reaction was stopped by adding 50 μ l of stopping solution. The optical density of the reaction was measured immediately at 450 nm. The standard curve was made by using the logarithm of the absorbance versus the concentrations of the standard. The minimum detectable dose of oxytocin is typically <4.99 pg/ml. It also has no cross-reaction with known neuropeptide including vasopressin.

To assay extracellular oxytocin levels in the incubation of the hypothalamus, hypothalamic blocks (4 \times 2.5 \times 2.5 mm, 20 mg) containing two SON and two paraventricular nuclei and their associated accessory nuclei were dissected from control and IPD dams and then separately incubated in the artificial cerebrospinal fluid (200 μ l, 35°C, 1 hr) in the presence of protease inhibitors (0.5 \times from a 100 \times stocking solution, P8340, Sigma-Aldrich, Shanghai, China) and 12 mM KCl in artificial cerebrospinal fluid. The solution was then frozen until assay as described earlier.

Whole-Cell Patch-Clamp Recordings

The electrical activity of oxytocin neurons was recorded in the SON in brain slices from male rats as previously described (Wang and Hatton, 2009b). Whole-cell patch-clamp recordings of oxytocin neurons were performed with patch pipette under the perfusion of 35°C artificial

cerebrospinal fluid via a gravity-fed perfusion system at 1.5 to 2 ml/min. Patch pipette-filling solution contained (in mmol/L) 145 K-gluconate, 10 KCl, 1 MgCl₂, 10 4-(2-Hydroxyethyl)piperazine-1-ethanesulfonic acid, N-(2-Hydroxyethyl)piperazine-N'-(2-ethanesulfonic acid), 1 Ethylene glycol-bis(2-aminoethylether)-N,N,N',N'-tetraacetic acid, 0.01 CaCl₂, 2 Mg-ATP, and 0.5 Na₂-GTP, pH 7.3, adjusted with KOH. In the recording, patch electrodes were guided onto the soma of SON neurons under visual observation through a microscope (Eclipse FN1, Nikon, Tokyo, Japan) equipped with an infrared camera and water-immersion objectives. The 700B amplifier (Molecular Devices, San Jose, CA, USA) was used for collecting electrical signals that were filtered and sampled at 5 kHz by Clampex 10 software through the 1550 analog-to-digital converter (Molecular Devices, San Jose, CA, USA). Data were stored in a computer for offline analysis.

For identifying the chemical nature of recorded neurons, 0.05% biocytin (B4261, Sigma-Aldrich, Shanghai, China) was added to the pipette solution. After recording, the slice was fixed with 4% paraformaldehyde for 4 hr, and the chemical nature of the recorded neurons was further identified as that described in the Immunohistochemistry section.

Data Analysis

Data analyses were similar to previous publications (Wang and Hatton, 2009b; Liu et al., 2019). In Western blots and coimmunoprecipitation, protein bands were quantified by multiplying average intensity and pixel numbers using Image J or Photoshop software, which was further corrected with the intensity of their corresponding loading control protein(s) and expressed as the percentage of controls. For coimmunoprecipitation, IgG (heavy chain) and total lysate were used as negative and positive controls, respectively. In analyzing data from patch-clamp recordings, Clampfit 10 software was used to detect firing rates, spike amplitude, width at 50% amplitude (half-width), and instantaneous frequency as well as the amplitude, half-width, and decay tau of the afterhyperpolarizing potential (AHP). A liquid junctional potential of -11 mV ~ -16 mV was left uncorrected. Data were stored in a computer for offline analysis.

Data were expressed as mean ± SEM. All the analyses were performed using Sigma Stat program (SPSS 19, Chicago, IL, USA) software. Student's *t* test was used for comparison between two groups; Chi-square test was used for comparison of the rate; analysis of variance (ANOVA) was used for comparison between multiple groups followed by Bonferroni (for normally distributed variables) and Dunnett's T3 test (intergroup comparison for not normally distributed variables) that were used for statistical analyses where appropriate as indicated in the

Results section. A value of *p* less than .05 was considered statistically significant.

Results

In this study, 42 lactating rats were used for behavioral observation and mechanistic analyses. In addition, 25 male rats were used for supplemental analyses of the interactions between OTR-associated signaling proteins and HCN3.

Lactation Performance

To clarify the effects of PD on maternal behavior at the middle stage of lactation, we observed dams' behaviors in IPD and CPD, respectively. In general, the litters in different groups had the same basal body weight before separating from the dams (175.9 ± 1.7 g, *n* = 14 in control; 181.3 ± 1.4 g, *n* = 14 in IPD, *p* = 1.000 by ANOVA; 184.4 ± 1.7 g, *n* = 14 in CPD, *p* = .946 to control by Bonferroni correction; Figure 1A). It indicates that the basal lactation performance was compared among different groups. Next, we analyzed the milk availability throughout IPD Day 1 to Day 4 (Figure 1B). On the first day of IPD, the LBWG was more than that in control group (11.3 ± 0.2 g, *n* = 14 in IPD vs. 3.3 ± 0.2 g, *n* = 14 in control, *p* = .00001 by Student's *t* test). Then, the LBWG gradually reduced from PD Day 2 (2.6 ± 0.3 g, *n* = 14 in IPD vs. 3.2 ± 0.2 g, *n* = 14 in control, *p* = .692 by Student's *t* test), to PD Day 3 (0.04 ± 0.2 g, *n* = 14 in IPD vs. 3.5 ± 0.1 g, *n* = 14 in control, *p* = .005 by Student's *t* test), and to PD Day 4 (-1.8 ± 0.2 g, *n* = 14 in IPD vs. 2.9 ± 0.2 g, *n* = 14 in control, *p* = .0004 by Student's *t* test).

Moreover, we analyzed suckling activity and LBWG during 1 hr observation at PD Day 5 and revealed significant difference in the LBWG between control, IPD, and CPD dams (*p* < .05 by ANOVA). That is, -1.3 ± 0.2 g, *n* = 13 in IPD versus 1.2 ± 0.2 g, *n* = 13 in control, *p* = .015 by Dunnett's T3 test; -1.6 ± 0.06 g, *n* = 12 in CPD, *p* = .007 to control by Dunnett's T3 test (Figure 1C). Consistently, the latency of suckling in PD group was longer (*p* < .05, by ANOVA), particularly in CPD (14.4 ± 0.7 min, *n* = 10 in IPD vs. 9.3 ± 0.5 min, *n* = 10 in control, *p* = .201 by Dunnett's T3 test; 28.0 ± 0.6 min, *n* = 10 in CPD, *p* = .0001 to control and *p* = .0001 to IPD by Dunnett's T3 test; Figure 1D). These findings are consistent with a previous report (Wang and Hatton, 2009a).

Maternal Interests to the Pups

Further observations revealed that the interests of PD dams toward the pups reduced significantly as shown in pup retrieval and anogenital licking (Figure 2). The number of pups retrieved was gradually reduced in IPD

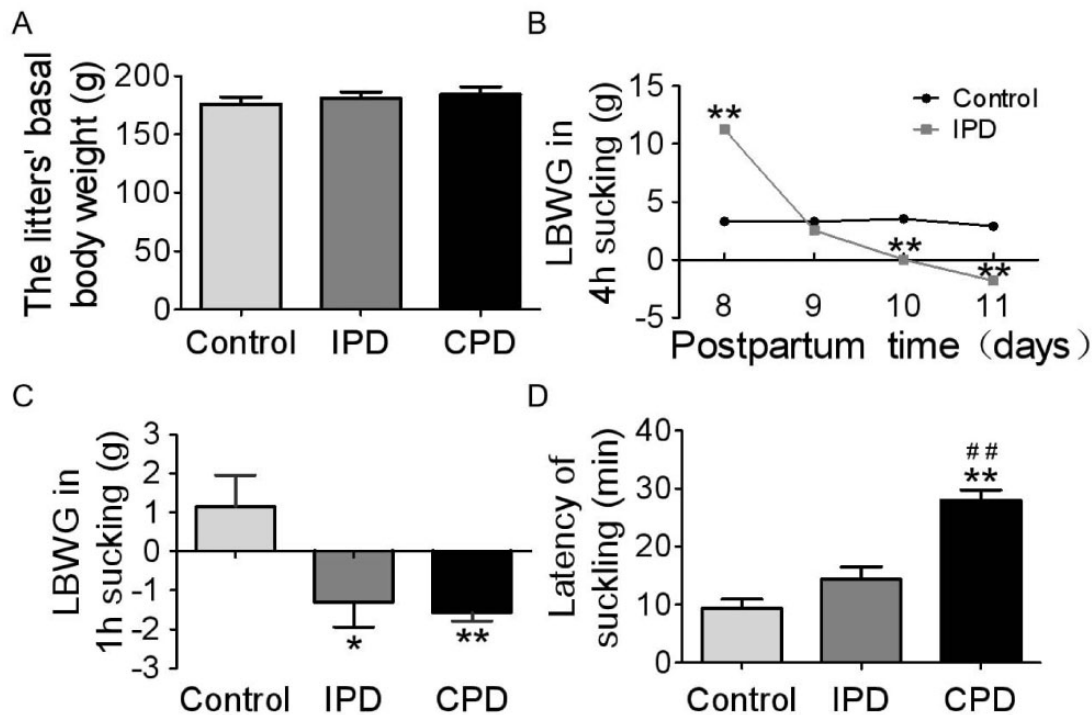


Figure 1. Effects of Pup Deprivation on Lactation Performance of Rat Dams. (A) Graphs summarizing the litters' basal body weight before separation. (B) Graphs summarizing the LBWG during 4 hr suckling from PD Day 1 to Day 4 ($n = 14$). (C) LBWG in 1 hr suckling at PD Day 5 ($n = 13$ in control, $n = 13$ in IPD, and $n = 12$ in CPD). (D) The latency of suckling in the first 30 min at PD Day 5 ($n = 10$). Data are shown as mean \pm SEM; * $p < .05$, ** $p < .01$ versus control by ANOVA; ## $p < .01$ versus IPD by ANOVA. CPD = continuous pup deprivation; IPD = intermittent pup deprivation; LBWG = litter's body weight gain.

and CPD groups. The number of dams retrieving pups reduced gradually from IPD to CPD (7/9 in IPD vs. 9/9 in control, $p = .134$ by Chi-square test; 2/9 in CPD, $p = .001$ to control and $p = .018$ to IPD by Chi-square test). CPD also significantly extended the latency of retrieval (12.1 ± 1.2 min in IPD vs. 1.9 ± 0.3 min in control, $p = .068$ by Dunnett's T3 test; 25.9 ± 0.9 min in CPD, $p = .0001$ to control and $p = .025$ to IPD by Dunnett's T3 test following ANOVA; $n = 9$, Figure 2A).

Consistently, the latency of anogenital licking was significantly longer in PD ($p < .05$, by ANOVA), particularly in CPD (3.7 ± 0.2 min, $n = 10$ in IPD vs. 3.3 ± 0.2 min, $n = 10$ in control, $p = .951$ by Dunnett's T3 test; 20.3 ± 1.1 min, $n = 10$ in CPD, $p = .003$ to control and $p = .003$ to IPD by Dunnett's T3 test; Figure 2B). Moreover, the number of licking in PD dams was significantly lower ($p < .05$, by ANOVA), particularly in CPD (13.5 ± 0.5 , $n = 10$ in IPD vs. 11.0 ± 0.5 , $n = 10$ in control, $p = .617$ by Dunnett's T3 test; 5.8 ± 0.7 , $n = 10$ in CPD, $p = .192$ to control and $p = .038$ to IPD by Dunnett's T3 test; Figure 2C). These changes are consistent with previous findings in rat dams with PD (Wang and Hatton, 2009a; Preckel and Kanske, 2018) and indicate reduction of maternal behavior.

In addition, we observed dams' self-grooming, a sign of social anxiety (Kalueff and Tuohimaa, 2004). The number of self-grooming in CPD dams was significantly higher than that in control dams (6.1 ± 0.2 , $n = 10$ in IPD vs. 3.5 ± 0.3 , $n = 10$ in control, $p = .068$ by Dunnett's T3 test; 12.6 ± 0.9 , $n = 10$ in CPD, $p = .026$ to control and $p = .120$ to IPD by Dunnett's T3 test; Figure 2D). These findings are consistent with previous report that mother–neonate separation is detrimental to the relationship between mothers and the babies (Bergman, 2019).

Effects of PD on the Development of Mammary Glands and Uterine Recovery

The breast is a pivotal interface of maternal–neonate interaction as the effector of the milk-ejection reflex. Thus, we analyzed their histological features (Figure 3A). Relative to the enlarged and well-differentiated alveoli in the control mammary glands, PD caused involution-like changes in the mammary glands because the percentage of alveolar area over the total glandular area decreased significantly ($p < .05$ by ANOVA). That is, $67.5 \pm 1.9\%$, $n = 5$ in IPD vs. $93.0 \pm 1.3\%$, $n = 5$ in control, $p = .004$ by Dunnett's T3 test;

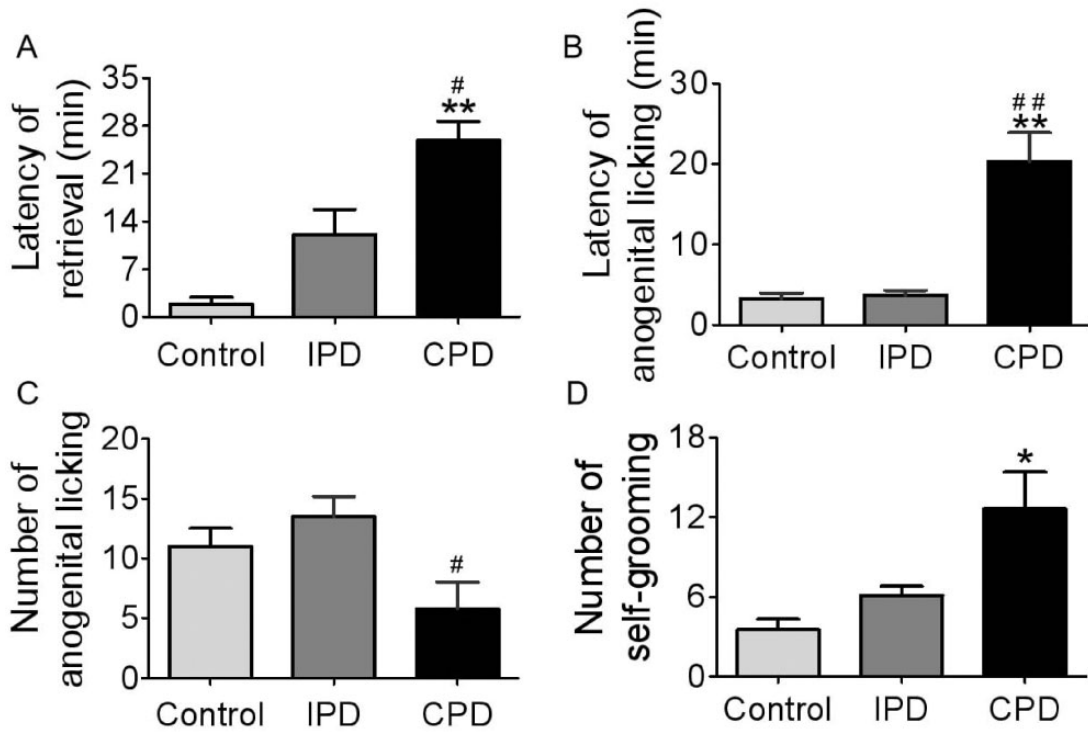


Figure 2. Effects of PD on Dams' Behavior. (A–D) Bar graphs summarizing the latency of pup retrieval (A, $n = 9$), latency (B, $n = 10$), and numbers (C, $n = 10$) of anogenital licking, and numbers of self-grooming (D, $n = 10$). $*p < .05$, $**p < .01$ versus control by ANOVA; $\#p < .05$, $\#\#p < .01$ versus IPD by ANOVA.

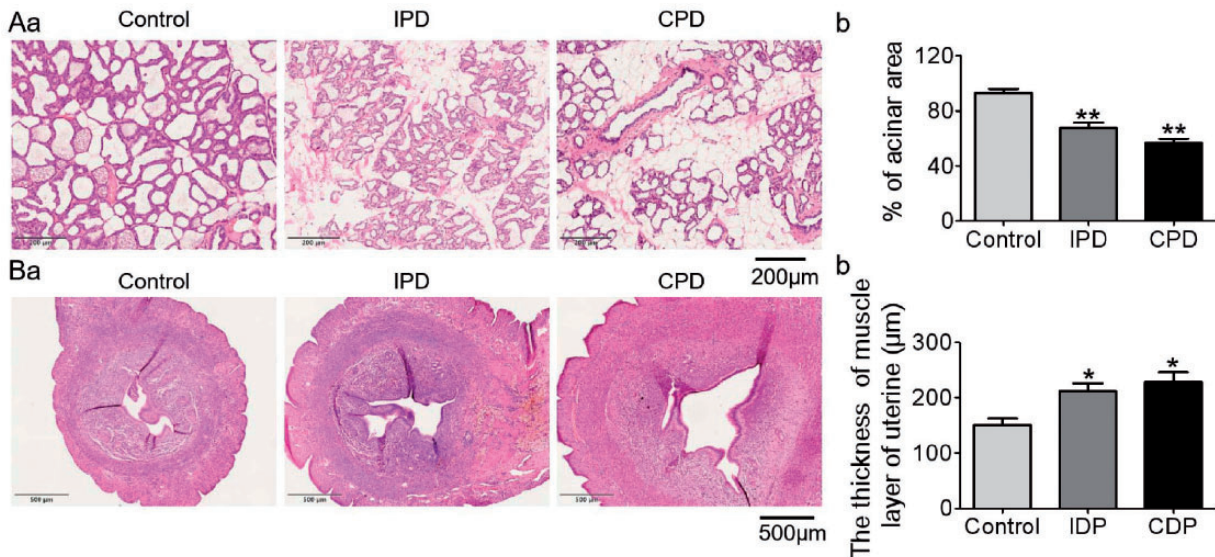


Figure 3. Effects of PD on the Histology of the Mammary Glands and Uteri. (A) Representative hematoxylin and eosin staining of five mammary glands (a) and bar graph summarizing the ratio of alveolar area versus total glandular area (b). (B) Representative hematoxylin and eosin staining of seven uteri in cross section (a) and bar graph summarizing the thickness of the uterine muscle layer (b). $*p < .05$, $**p < .01$ versus control by ANOVA.

$56.6 \pm 1.4\%$, $n = 5$ in CPD, $p = .0001$ to control and $p = .182$ to IPD by Dunnett's T3 test.

Along with the changes in the mammary glands, postpartum recovery of the uterus depends on the

milk-ejection reflex-associated bolus oxytocin release. Thus, we examined the histological feature of the uterus of PD dams. As shown in Figure 3B, the thickness of the uterine muscle layer increased significantly in PD

dams ($p < .05$ by ANOVA). That is, $211.6 \pm 5.3 \mu\text{m}$, $n = 7$ in IPD versus $150.6 \pm 4.5 \mu\text{m}$, $n = 7$ in control, $p = .018$ by Dunnett's T3 test; $228.3 \pm 6.8 \mu\text{m}$, $n = 7$ in CPD, $p = .013$ to control and $p = .846$ to IPD by Dunnett's T3 test. Correspondingly, the area of uterine cavity became larger in the PD dams, particularly in the CPD group. These results indicate that PD causes early involution of the mammary glands and delays the recovery of uterus and support the hypothesis that PD causes the failure of milk-ejection reflex-associated bolus release of oxytocin (Hatton and Wang, 2008).

Concentration of Oxytocin in the Hypothalamus and Blood

Our preliminary study has revealed that IPD caused failure of the burst discharges in oxytocin neurons during suckling (Wang and Hatton, 2009a), while oxytocin neurons presented depolarization in the membrane potential in IPD dams (Liu et al., 2016). It is likely that oxytocin secretion in the hypothalamus was different from that in the posterior pituitary, and thus, we further examined hypothalamic oxytocin secretion and plasma oxytocin levels. The hypothalamic explants were incubated in the presence of 12 mM K^+ and protease inhibitor for 1 hr, and the incubation media were collected for assaying oxytocin levels. The concentration of oxytocin in hypothalamus increased in IPD group compared with the control ($51.8 \pm 1.5 \text{ pg/mg}$ in IPD vs. $21.3 \pm 1.0 \text{ pg/mg}$ in control, $p = .0001$ by Student's t test; $n = 6$, Figure 4A). The high level of hypothalamic oxytocin secretion is in agreement with the depolarization of oxytocin neurons in PD dams (Liu et al., 2016).

Moreover, we sampled blood from dams at 30 min after separating the litters from dams at PD Day 5 and assayed plasma oxytocin levels. The results revealed that there was no significant difference in plasma oxytocin concentrations among the three groups ($323.0 \pm 6.3 \text{ pg/}$

ml, $n = 8$ in control, $343.6 \pm 9.2 \text{ pg/ml}$, $n = 8$ in IPD, $p = .742$ to control by Bonferroni correction; $359.6 \pm 7.3 \text{ pg/ml}$, $n = 8$ in CPD, $p = .742$ to control by Bonferroni correction; Figure 4B). This finding suggests that breastfeeding failure was not due to low basal blood oxytocin levels but because of failure in bolus release of oxytocin in PD dams.

Activity of SON Neurons in PD Dams

To identify whether the hypogalactia in PD dams was associated with reduced activity of oxytocin neurons, we analyzed the expressions of c-Fos and pERK1/2, the two biomarkers of oxytocin neuronal activity. The expressions of c-Fos increased in PD dams ($p < .05$, ANOVA) in the SON by Western blots, particularly in CPD ($109.9 \pm 3.9\%$ of the control, $n = 6$ in IPD, $p = 1.000$ to control by Dunnett's T3 test; $129.5 \pm 6.3\%$ of the control, $n = 6$ in CPD, $p = .046$ to control by Dunnett's T3 test; Figure 5A). However, pERK1/2 levels in PD did not differ significantly from the control ($108.9 \pm 2.5\%$ of the control, $n = 7$ in IPD, $p = .111$ to control by Bonferroni correction, and $120.6 \pm 3.6\%$ of the control, $n = 7$ in CPD, $p = .134$ to control by Bonferroni correction; Figure 5B). These findings are in agreement with IPD-evoked reduction of firing activity in oxytocin neurons and the intermittent increases in the intramammary pressure (Liu et al., 2016).

HCN3 Expressions in PD Dams

Observations presented earlier suggest central disorder in oxytocin secretion of PD dams. To explore the paradoxical hypothalamic and pituitary oxytocin secretions, we analyzed the association of OTR-associated signaling events with the expression of HCN3. As shown in Figure 6, HCN3 was specifically expressed on oxytocin neurons in immunohistochemistry. There was no significant difference in the number of HCN3-expressing oxytocin neurons between the three groups

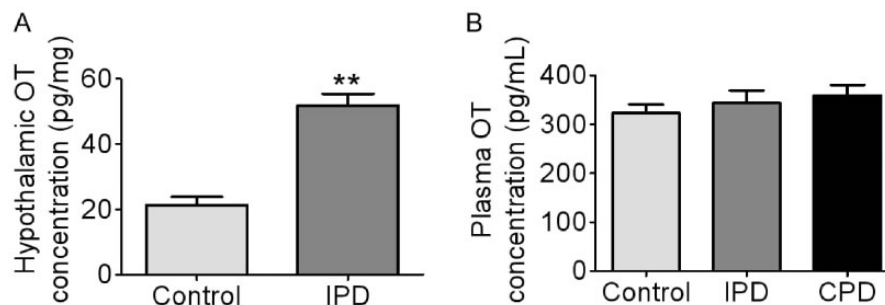


Figure 4. Levels of OT in the Hypothalamus and the Plasma. (A) OT in the incubation medium of the hypothalamic blocks ($n = 6$). (B) Plasma OT concentration at PD Day 5 ($n = 7$). $**p < .01$ versus control by Student's t test. IPD = intermittent pup deprivation; CPD = continuous pup deprivation; OT = oxytocin.

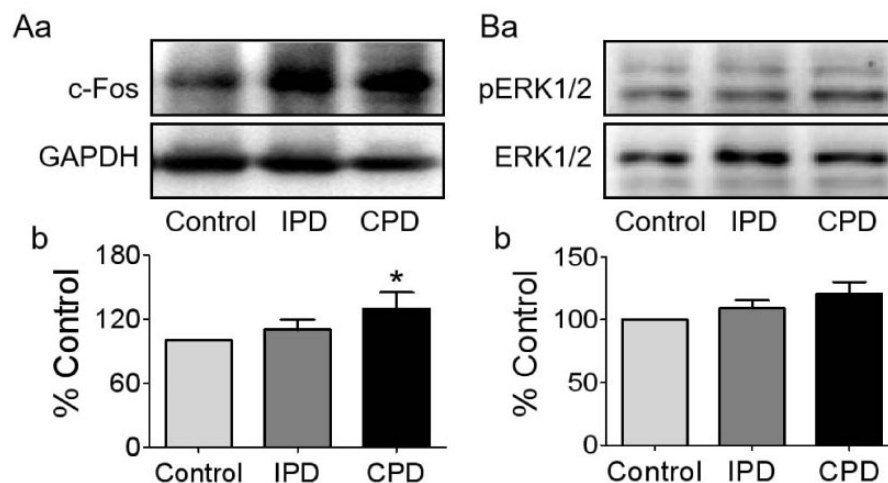


Figure 5. Effects of PD on the Expression of c-Fos and pERK1/2 in the Supraoptic Nucleus (SON). (A and B) Western blotting bands (a) and their statistical analyses (b) of c-Fos (A, $n = 6$) and pERK1/2 (B, $n = 7$). * $p < .05$ versus control by ANOVA. pERK1/2 = phosphorylated extracellular signal-regulated protein kinase 1/2; IPD = intermittent pup deprivation; CPD = continuous pup deprivation; GAPDH = glyceraldehyde 3-phosphate dehydrogenase.

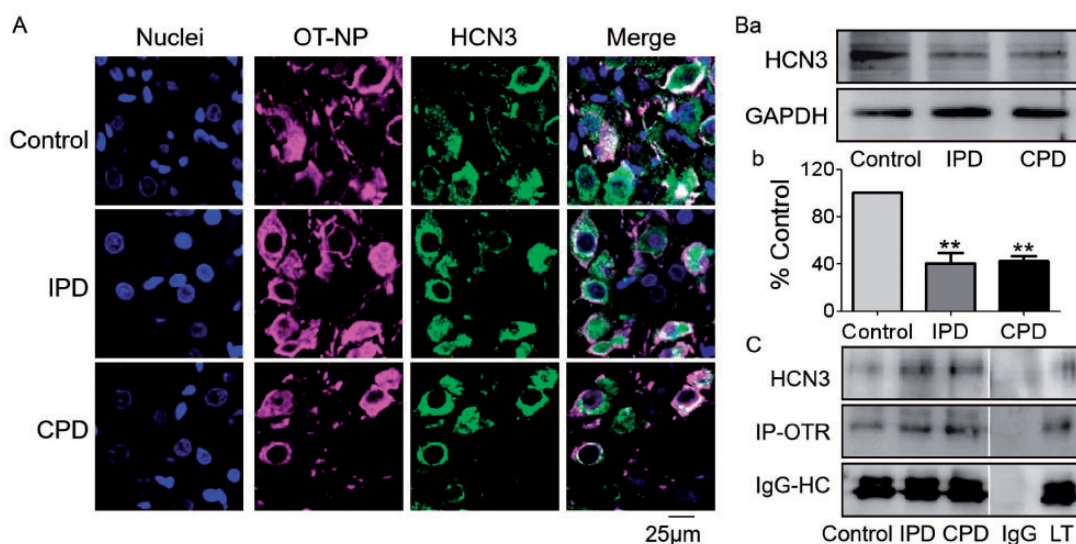


Figure 6. Effects of PD on the Expression of HCN3 in the SON. (A) Representative fluorescent images of nuclei (in blue), OT-NP (in magenta), HCN3 (in green) and their merges ($n = 4$ in control, $n = 5$ in IPD, and $n = 4$ in CPD). (B) Western blotting bands (a) and the summary graph (b) ($n = 6$). (C) Protein bands showing coimmunoprecipitation of OTR with HCN3. The noncontiguous gel lanes are reassembled from two sections of the same protein membrane after removal of irrelevant bands. Note: IgG and total lysate (TL): negative and positive controls, respectively; IgG-HC, IgG heavy chain. ** $p < .01$ versus control by ANOVA.

HCN3 = hyperpolarization-activated cyclic nucleotide-gated channel 3; IPD = intermittent pup deprivation; CPD = continuous pup deprivation; OT-NP = oxytocin-neurophysin; GAPDH = glyceraldehyde 3-phosphate dehydrogenase; OTR = oxytocin receptor.

($n = 4$). Further quantitating HCN3 expression in Western blots revealed that HCN3 decreased significantly in the SON in both IPD and CPD ($40.3 \pm 3.6\%$ of the control, $n = 6$ in IPD, $p = .003$ to control by Dunnett's T3 test; $42.1 \pm 1.8\%$ of the control, $n = 6$ in CPD, $p = .0001$ to control by Dunnett's T3 test; Figure

6B). In coimmunoprecipitation, molecular association between OTR and HCN3 was identified (Figure 6C), which clearly increased in three IPD dams (118.6%, 175.4%, and 133.6% of control) and was relatively diverse in CPD dams (758.5%, 106.7%, and 104.1% of control). These findings suggest that OTR-HCN3 signaling is associated with oxytocin neuronal activity.

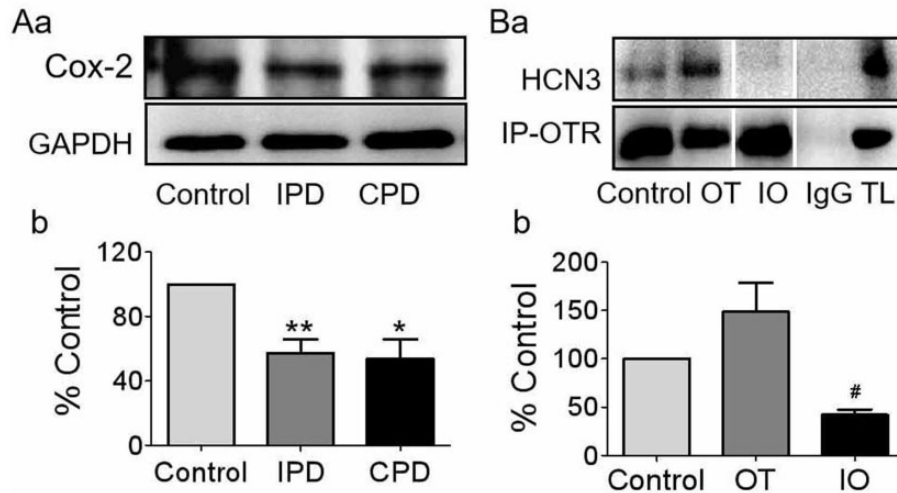


Figure 7. Effects of PD on the Expressions of Cox-2 and its Influences on OT-Modulated Molecular Association Between OTR and HCN3 in the SON. (A) Western blotting bands (a) and the summary graphs (b) displaying PD effects on the expression of Cox-2 ($n=7$). (B) Representative protein bands showing coimmunoprecipitation of OTR with HCN3 in the SON of brain slices (a) and the summary graph (b, $n=4$), respectively. The noncontiguous gel lanes are reassembled from two sections of the same protein membrane after removal of irrelevant bands. # $p < .05$ compared with OT by ANOVA. * $p < .05$, ** $p < .01$ versus control by ANOVA. HCN3 = hyperpolarization-activated cyclic nucleotide-gated channel 3; IPD = intermittent pup deprivation; CPD = continuous pup deprivation; GAPDH = glyceraldehyde 3-phosphate dehydrogenase; Cox-2 = cyclooxygenase-2; OT = oxytocin; IO = indomethacin + oxytocin; TL = total lysate; OTR = oxytocin receptor.

Involvement of HCN3 in the Firing Activity of Oxytocin Neurons

In suckling activation of oxytocin neurons, induction of cyclooxygenase-2 and the ensuing production of PGE₂ (Wang and Hatton, 2006) are essential events for burst generation (Wang et al., 2016). Thus, we assayed the expression of cyclooxygenase-2 in the SON of PD dams in Western blots (Figure 7A). Cyclooxygenase-2 decreased significantly ($p < .05$ by ANOVA) in both IPD and CPD dams ($57.4 \pm 3.2\%$ of the control, $n=7$ in IPD, $p = .007$ to control by Dunnett's T3 test; $53.6 \pm 4.6\%$ of the control, $n=7$ in CPD, $p = .025$ to control and $p = .991$ to IPD by Dunnett's T3 test). This is consistent with the role of PGE₂ in the activation of oxytocin neurons (Hatton and Wang, 2008) and PD-evoked milk-ejection reflex failure (Liu et al., 2016).

Next, we performed coimmunoprecipitation *in vitro* to identify the potential association between downstream signaling molecules of OTR and HCN3 in the SON following oxytocin treatments without or with indomethacin (Figure 7B). Based on the rule of minimizing sacrifice in studies using animals and the similarity of the electrical features between lactating and male (but not virgin female) rats (Wang and Hatton, 2005), we used the SON from male rats. There was no significant difference in the expression of OTR between different groups. Oxytocin tended to increase the molecular association between OTR and HCN3 and that was reversely reduced by indomethacin ($148.7 \pm 15.0\%$ of control in oxytocin, $n=4$,

$p = 1.000$ compared with the control; $42.0 \pm 2.8\%$ of control in indomethacin+oxytocin, $n=4$, $p = .089$ to the control and $p = .030$ to oxytocin by Dunnett's T3 test). This finding is consistent with the mediating role of prostaglandins in oxytocin-evoked burst firing in oxytocin neurons (Wang et al., 2016).

To test if PGE₂ mediation of oxytocin-evoked burst discharge (Wang and Hatton, 2006) was achieved by activating HCN3, we further observed effects of HCN3 blockade on PGE₂-evoked excitation of oxytocin neurons in the SON of brain slices from male rats. As shown in Figure 8A, PGE₂ (0.1 $\mu\text{mol/L}$, 10 min) significantly increased the firing rate (Figure 8Aa), and changed spike duration (Figure 8Ab) in oxytocin neurons. In these PGE₂ effects, the firing rate in oxytocin neurons was increased significantly (9.1 ± 0.3 Hz, $n=10$ in PGE₂ vs. 6.5 ± 0.2 Hz before PGE₂, $n=10$, $p = .047$ by paired t test; Figure 8Ac); the half-width of spikes was widened (2.9 ± 0.04 ms, $n=10$ in PGE₂ vs. 2.5 ± 0.04 ms, $n=10$ before PGE₂, $p = .045$ by paired t test; Figure 8Ad); and the instantaneous firing rate also tended to increase (9.3 ± 0.3 Hz, $n=10$ in PGE₂ vs. 7.1 ± 0.2 Hz, $n=10$ before PGE₂, $p = .100$ by paired t test; Figure 8Ae). Moreover, the amplitude of AHP decreased significantly (-12.3 ± 0.3 mV, $n=10$ in PGE₂ vs. -9.1 ± 0.3 mV, $n=10$ before PGE₂, $p = .049$ by paired t test; Figure 8Bb). However, there was no significant change in the half-width of AHP (26.7 ± 1.0 ms, $n=10$ in PGE₂ vs. 28.2 ± 0.9 ms, $n=10$ before PGE₂, $p = .570$ by paired t test; Figure 8Bc) or the decay tau (45.1 ± 2.7 ms, $n=10$ in

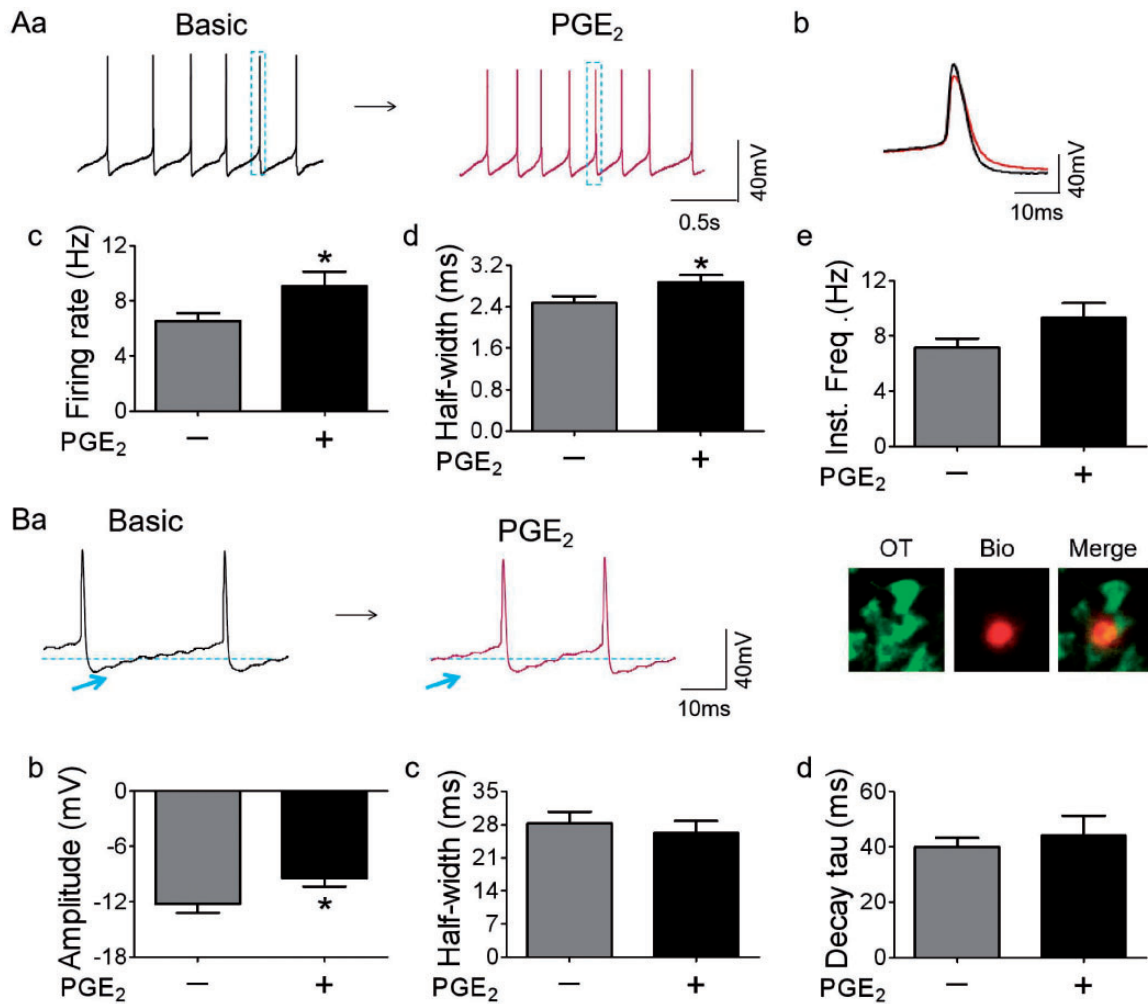


Figure 8. PGE₂-Evoked Excitation in OT Neurons in the SON. (A) Effects of PGE₂ ($n = 10$): exemplary tonic firing episodes (control in black, and PGE₂ in magenta; Aa), single spikes (Ab), and the bar graphs summarizing effects of PGE₂ on the firing rate (Ac), the half-width of spikes (Ad), and the instantaneous firing rate (Ae). The inset at the right side is a set of representative images of a chemically identified OT neuron labeled with biotin during recording. (B) Effects of PGE₂ on AHP (below the dashed line, arrow) of OT neurons (Ba) and the bar graphs summarizing the effects of PGE₂ on the amplitude (Bb, $n = 10$), half-width (Bc, $n = 10$), and the decay tau (Bd, $n = 10$). * $p < .05$ versus before PGE₂ by paired t test. OT = oxytocin; PGE₂ = prostaglandin E₂.

PGE₂ vs. 39.9 ± 1.2 ms, $n = 10$ before PGE₂, $p = .605$ by paired t test; Figure 8Bd).

Then, we blocked HCN3 by using DK-AH269 (Neitz et al., 2011; Lu et al., 2020) and then tested effects of PGE₂ on the electrical activity of oxytocin neurons (Figure 9A). DK-AH269 (10 μ mol/L) significantly reduced the firing rate (5.9 ± 0.5 Hz, $n = 10$ in DK-AH269 vs. 11.1 ± 0.4 Hz, $n = 10$ before DK-AH269, $p = .047$ by Dunnett's T3 test) and blocked PGE₂-evoked increase in the firing rate (4.0 ± 0.6 Hz, $n = 9$ in DK-AH269 + PGE₂, $p = .775$ to DK-AH269 by Dunnett's T3 test; Figure 9Ac). DK-AH269 did not significantly influence half-width of the spike (3.0 ± 0.08 ms, $n = 10$ in DK-AH269 vs. 2.7 ± 0.06 ms, $n = 10$ before DK-AH269, $p = 1.000$ by Bonferroni correction) and

the instantaneous firing rate (4.1 ± 0.2 Hz, $n = 10$ in DK-AH269 vs. 6.2 ± 0.2 Hz, $n = 10$ before DK-AH269, $p = .115$ by Bonferroni correction). In the presence of DK-AH269, PGE₂ did not influence spike half-width (3.6 ± 0.3 ms, $n = 5$, $p = .444$ to DK-AH269 by Bonferroni correction; Figure 9Ad) and the instantaneous firing rate (4.1 ± 0.4 Hz, $n = 6$, $p = 1.000$ to DK-AH269 by Bonferroni correction; Figure 9Ae). Moreover, in the presence of DK-AH269 without or with PGE₂, there were no significant changes in the amplitude of AHP (-7.4 ± 0.1 mV, $n = 10$ in DK-AH269 vs. -7.7 ± 0.1 , $n = 10$ before DK-AH269, $p = 1.000$ by Bonferroni correction; -6.1 ± 0.5 mV, $n = 5$, in DK-AH269 + PGE₂, $p = .596$ to DK-AH269 by Bonferroni correction; Figure 9Bb), the half-width

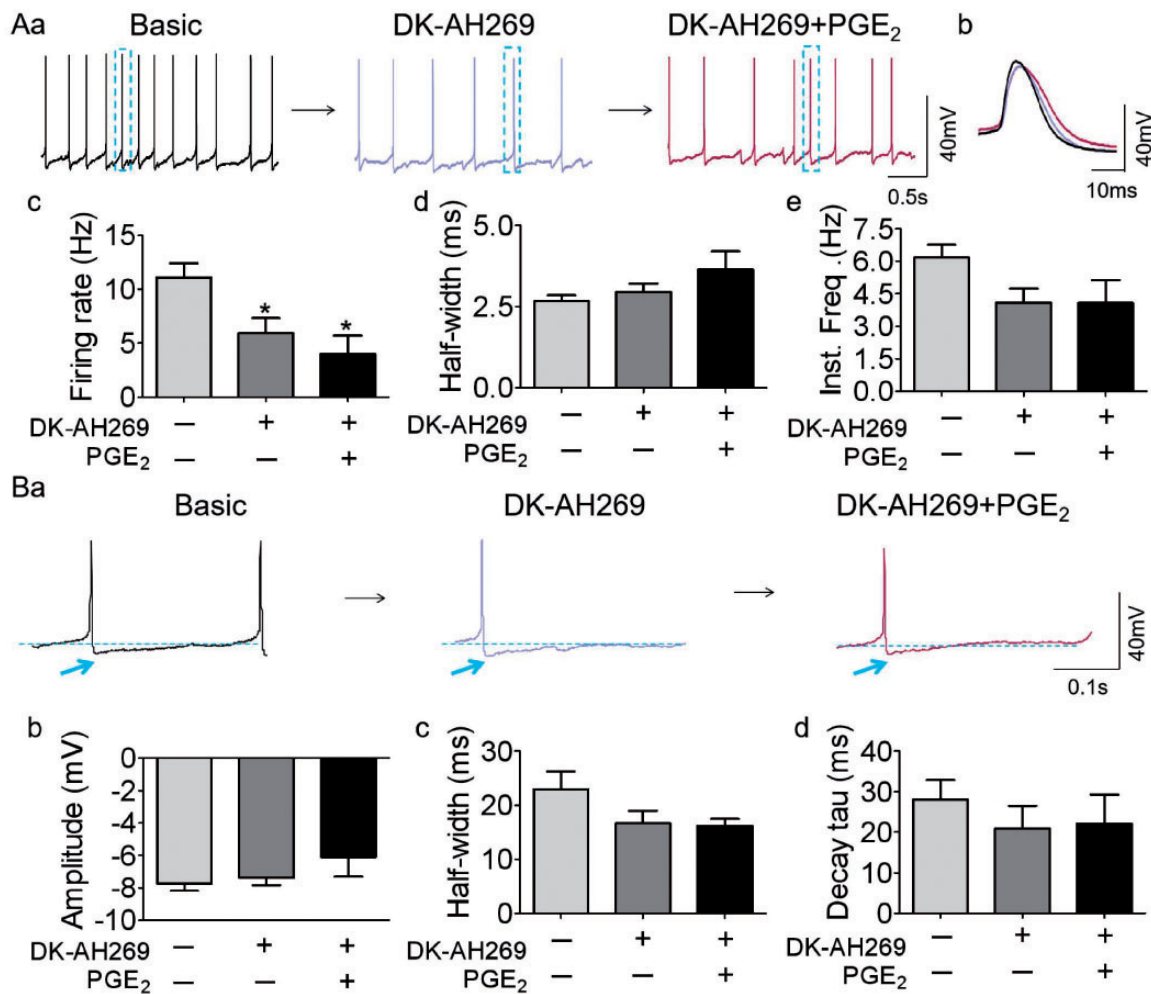


Figure 9. HCN3 Mediation of PGE₂-Evoked Excitation and Burst Discharges in OT Neurons. (A) Effects of HCN3 inhibitor, DK-AH269, on PGE₂ effects: exemplary firing episodes (a) and the summary (c–e). Note that, $n = 10$ before DK-AH269, $n = 10$ in DK-AH269, and $n = 6$ in DK-AH269 + PGE₂. (B) Effect of DK-AH269 and PGE₂ on AHP of OT neurons (Ba) and the summary in bar graphs (b–d). Note that, $n = 10$ before DK-AH269, $n = 10$ in DK-AH269, and $n = 5$ in DK-AH269 + PGE₂. * $p < .05$ versus before DK-AH269 by ANOVA. HCN3 = hyperpolarization-activated cyclic nucleotide-gated channel 3; OT = oxytocin; PGE₂ = prostaglandin E₂.

of AHP (20.4 ± 1.2 ms, $n = 10$ in DK-AH269 vs. 23.0 ± 1.0 ms, $n = 10$ before DK-AH269, $p = 1.000$ by Bonferroni correction; 19.4 ± 1.5 ms, $n = 5$, in DK-AH269 + PGE₂, $p = 1.000$ DK-AH269 by Bonferroni correction; Figure 9Bc), and the decay tau (20.9 ± 1.8 ms, $n = 10$ in DK-AH269 vs. 28.1 ± 1.5 ms, $n = 10$ before DK-AH269, $p = 1.000$ by Bonferroni correction; 22.1 ± 3.2 ms, $n = 5$, DK-AH269 + PGE₂, $p = 1.000$ to DK-AH269 by Bonferroni correction; Figure 9Bd). The blocking effect of DK-AH269 on PGE₂-evoked excitation of oxytocin neurons is consistent with its reduced expression in PD dams.

Discussion

In the present study, we identified that PD causes abnormal postpartum maternal behavior and hypogalactia.

These effects are related to increase in oxytocin synthesis and secretion in the hypothalamus and decrease in the burst firing ability of oxytocin neurons. At molecular levels, these changes are associated with reduced cyclooxygenase-2 induction and the ensuing PG activation of HCN3. These findings provide new insights into the cellular mechanisms underlying the activation of oxytocin neurons and abnormal oxytocin neuronal activity in mothers separated from their babies.

Maternal Behavior and Lactation Performance

The present study reveals that PD can cause hypogalactia, depressive-like maternal behavior, and anxiety. The severity of these effects is related to the extents of PD. This finding is consistent with previous reports about

IPD effects at early (Liu et al., 2019) or middle stage of lactation (Wang and Hatton, 2009a; Liu et al., 2016).

The abnormal maternal behavior can result from separation stress and lack of suckling stimulation. Suckling-evoked oxytocin release is essential for positive maternal mood. However, separation from the offspring could evoke a series of stress reaction by increasing sympathetic output and activating the hypothalamic-pituitary adrenal axis (van Bodegom et al., 2017). Resultantly, the “defense system” built on the antidepressive and anxiolytic effects of endogenous oxytocin is disrupted (Li et al., 2016). By contrast, lack of suckling stimulation can cause milk accumulation in the mammary glands, inhibit the secretion of prolactin, and suppress milk production and secretion, thereby leading to *no milk* for the sucking pups (Liu et al., 2016).

Notably, IPD at PD Day 1 can increase maternal behavior and lactation efficiency. This is in agreement with the common practice in studying on the milk-ejection reflex. That is, separating rat dams and their litters for several hours to overnight increases the probability of the milk-ejection reflex (Wang et al., 1995). It also matches the general regulation that lack of agonist (i.e., oxytocin) can sensitize the corresponding receptor (i.e., OTR) in short term, thereby increasing the biological reactions (i.e., the milk-ejection reflex).

PD Effects and the Activity of Oxytocin Neurons

In the present study, CPD significantly increased the expressions of c-Fos in the SON, which indicates increases in cellular activity (Morgan and Curran, 1991). This finding matches the increased secretion of hypothalamic oxytocin. The increase in hypothalamic oxytocin can increase the firing activity of oxytocin neurons and oxytocin release in both the brain and the posterior pituitary. However, prolonged oxytocin actions for days could reverse such excitatory effect due to an post-excitation inhibition as shown in lactating rats (Wang et al., 2006) and the depolarized membrane potential in oxytocin neurons in IPD dams (Liu et al., 2016) as well as the time-dependent change in LBWG.

Because there was no reduction in the basal level of plasma oxytocin in PD dams, we have to consider disorders in the patterns of oxytocin release from the posterior pituitary rather than its tonic release. This probability is supported by the following findings. That is, the early involution-like changes in the mammary glands and poor recovery of the uterus point to a common etiology that these OTR-bearing organs receive less stimulation from a pulsatile oxytocin (Uvnas-Moberg and Eriksson, 1996), a feature of oxytocin secretion from oxytocin neuronal terminals during lactation (Lincoln et al., 1973; Hatton and Wang, 2008). Because the bolus release of oxytocin is determined by burst discharge in oxytocin

neurons during the milk-ejection reflex (Hatton and Wang, 2008), the hypogalactia is due to failure in the burst discharge in oxytocin neurons during suckling stimulation in PD dams.

Similarly, the reduction in maternal behavior can also be attributable to the failure of burst-like firing activity of oxytocin neurons. In the brain, oxytocin can be released into the brain from axonal collaterals and into the hypothalamus from cell bodies and dendrites (Hou et al., 2016). Oxytocin releasing into the brain can regulate maternal behavior via projections to the bed nucleus of the stria terminalis, the medial prefrontal cortex, paraventricular nucleus, olfactory bulb, amygdala, and others (Jurek and Neumann, 2018). As reported, the pulsatility of oxytocin release is more closely related to the social desirability of mothers than tonic oxytocin release does (Nissen et al., 1998). In the failure of the milk-ejection reflex, bolus release of oxytocin into the brain from axonal collaterals should also be reduced. Thus, these social brain regions could not receive appropriate oxytocin actions, thereby disrupting maternal behavior while causing anxiety.

PGE₂, HCN3, and Oxytocin Neuronal Activity

At molecular levels, suckling-/oxytocin-evoked activation of oxytocin neurons in burst discharge depends on the induction of cyclooxygenase-2 (Hatton and Wang, 2008). PGE₂, a product of cyclooxygenase-2, has been identified as a key mediator in oxytocin-evoked burst discharge in oxytocin neurons in our previous study (Wang et al., 2016). Thus, the reduced expression of cyclooxygenase-2 and subsequent reduction of PG production could account for the loss of burst ability in oxytocin neurons and hypogalactia in PD dams (Wang and Hatton, 2009a; Liu et al., 2016). The reduced cyclooxygenase-2 could result from uncoupling of OTR with its early downstream signals, such as Gq protein and pERK1/2 in PD dams (Wang and Hatton, 2009a). Hence, the reduction of cyclooxygenase-2 expression is a pivotal link in OTR-associated signaling leading to the hypogalactia.

In the regulation of oxytocin neuronal activity, HCN3 is a key ion channel for suckling/oxytocin-evoked burst discharge in oxytocin neurons. As reported, the activity of HCN channels is associated with oxytocin secretion (Qiu et al., 2005; Pires da Silva et al., 2016). In the present study, we further identified that HCN3 was mainly expressed in oxytocin neurons and PD reduced the expression of HCN3 in the SON. Moreover, blocking HCN3 blocked PGE₂-evoked burst discharges. These findings clearly support that HCN3 plays a pivotal role in the burst firing in oxytocin neurons and that its down-regulation or inhibition leads to the failure of burst firing.

Between OTR and HCN3, PGE₂ can be a key mediator. In the present study, we found that DK-AH269

blocked PGE₂-evoked increases in the firing rate, the instantaneous firing rate, and the burst discharge and that indomethacin reduced oxytocin-evoked increase in the molecular association between OTR and HCN3. Thus, cyclooxygenase-2 and PGE₂ can mediate OTR-associated activation of HCN3 and the subsequent burst firing in oxytocin neurons.

The activation of HCN by prostaglandins has been identified extensively in previous studies. For example, the current density of HCN channels and intracellular Ca²⁺ concentration of the bladder were enhanced by sulprostone, a selective agonist of EP₃ (a receptor of PGE₂), or PGE₂; their effects were inhibited by ZD7288 (antagonist of HCN channels) treatment (Alotaibi et al., 2017). In small dorsal root ganglia neurons, PGE₂ can increase HCN-mediated current and the overall neuronal excitability (Resta et al., 2016). Together with these findings, our study for the first time indicates that the burst-evoking effect of PGE₂ is associated with the activation of HCN3.

In oxytocin regulation of the burst discharges of oxytocin neurons, cAMP can be a mediator between PGE₂ and HCN3. In the regulation of cellular excitability, cAMP has been identified extensively as a mediator between PGE₂ and HCN3. In small dorsal root ganglia neurons, PGE₂-evoked activation of HCN-mediated current and depolarization of resting membrane potential via EP₃ (Sachs et al., 2009) is inhibited by activation of GPR35, a Gi/o-coupled receptor that reduces intracellular cAMP levels (Resta et al., 2016). It is known that

cAMP can bind to the cyclic nucleotide-binding domain of the HCN3 (Akimoto et al., 2018) and activate it (Robichaux and Cheng, 2018). In our preliminary study, we have found that PD reduces the expression of catalytic subunit of protein kinase A in oxytocin neurons (Li et al., unpublished data). Thus, the loss of burst discharges in oxytocin neurons in PD dams could be due to reduced PG production following the downregulation of cyclooxygenase-2 and the ensuing suppression of prostaglandin-EP receptor-cAMP-HCN3 signaling pathway (Figure 10).

HCN3 Activity and Oxytocin Neuronal Activity

The contradiction of increased hypothalamic oxytocin secretion with milk-ejection reflex failure may reflect the differential effects of OTR-associated HCN3 on Ca²⁺ influx and on the firing activity/excitability. Oxytocin-evoked activation of HCN3 can increase Ca²⁺ influx to promote somatodendritic oxytocin release (Tobin et al., 2011). This is supported by the finding that blocking HCN3 also reduces PGE₂-evoked spike width increase (Figure 9Ad), an indicator of increase in Ca²⁺ influx. By contrast, PD also causes strong depolarization of the membrane potential (Liu et al., 2016), an effect similar to the prolonged action of oxytocin on oxytocin neurons (Wang et al., 2006). It is likely that the long increase in hypothalamic oxytocin level reduces functional HCN3 due to an internalization and desensitization along with its associated OTR. Resultantly, due to the reduction of

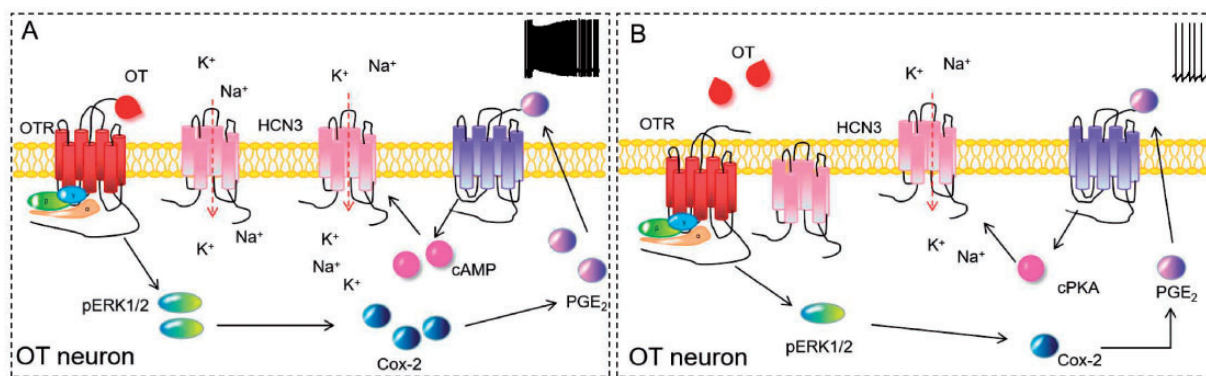


Figure 10. Diagram of the HCN3-Associated Cellular Mechanisms Underlying the Activation of OT Neurons and its Malfunction.

(A) Normal mother–baby interaction activates OTR and its downstream signals like pERK1/2 and cyclooxygenase-2. Cyclooxygenase-2 increases PGE₂ production that activates PG receptor (EP) and then the HCN3, likely mediated by cAMP that can bind to cyclic nucleotide-binding domain site of HCN3. The activation of HCN3 causes burst discharge through a rebound excitation. (B) PD causes increases in hypothalamic release of oxytocin that abnormally activates OTR. The overactivation of OTR also causes its internalization and increases molecular association with HCN3 in the cytosolic compartment. This subsequently downregulates cyclooxygenase-2 and HCN3, resulting in failure of burst discharge. The loss of burst discharge ability reduces oxytocin release into the brain and blood, thereby causing the reduction of maternal interest to the offspring, anxiety, and hypogalactia.

OT = oxytocin; Cox-2 = cyclooxygenase-2; PGE₂ = prostaglandin E₂; OTR = oxytocin receptor; cAMP = cyclic adenosine monophosphate; pERK1/2 = phosphorylated extracellular signal-regulated protein kinase1/2; HCN3 = hyperpolarization-activated cyclic nucleotide-gated channel 3; cPKA = catalytic subunit of protein kinase A.

HCN3 expression (Figure 6Ba) and/or activity, the excitability including burst firing ability in oxytocin neurons decreases (Wang and Hatton, 2009a).

Notably, PD increased molecular association of OTR with HCN3 in CPD dams as well as in oxytocin-treated SON. This finding is in agreement with the increased hypothalamic oxytocin secretion but seems contradictory with the reduced HCN3 expression and burst ability. However, based on previous findings (Wang and Hatton, 2009a; Liu et al., 2016), we tentatively believe that PD-evoked OTR expression (Wang and Hatton, 2009a) can increase its association with HCN3 directly or via cytoskeletal elements, which increases oxytocin neuronal activity; however, prolonged increase in hypothalamic oxytocin levels causes significant depolarization of the membrane potential, which weakens HCN3 expression and blocks burst firing. Although it remains to measure HCN3 current directly and evaluate the relative contributions of different types of ion channels, current findings allow us to propose such a differential regulating model for the brain effect and for the peripheral action. In addition, AHP seems having no remarkable effect on the contribution of HCN3 to PGE₂-associated burst discharges although blocking HCN3 also weakens PGE₂-evoked reduction of AHP amplitude.

Taken together, this study reveals for the first time that there is an OTR-PG-HCN3 signaling pathway in the regulation of oxytocin neuronal activity during suckling. PD disrupts maternal behavior including paradoxically increasing secretory activity of oxytocin neurons in the SON but reducing pulsatile oxytocin release from axonal terminals via inhibiting the activity of HCN3. Because oxytocin has extensive physiological and pathological functions (Whitley et al., 2019), further identification of the mechanisms underlying oxytocin neuronal activity undoubtedly contributes to the health of mothers.

Acknowledgments

The authors thank Drs. Runsheng Jiao and Jiao Wang for technique-related advices, Yang Liu for assistance in confocal imaging work, and Dan Cui and Jiawei Yu for critical reading.

Author Contributions

D. L., H. L., and H. W. collected and/or analyzed data. D. L. wrote the first draft of this article. All authors participated in the discussion and revision. Y.-F. W. and P. W. conceived the study, and Y.-F. W. made the final revision.

Declaration of Conflicting Interests

The author(s) declared no potential conflicts of interest with respect to the research, authorship, and/or publication of this article.

Funding

The author(s) disclosed receipt of the following financial support for the research, authorship, and/or publication of this article: This work was supported by the National Natural Science Foundation of China (grant no. 31471113, YFW), the fund of “Double-First-Class” Construction of Harbin Medical University (key laboratory of preservation of human genetic resources and disease control in China).

ORCID iD

Yu-Feng Wang  <https://orcid.org/0000-0001-8543-8906>

References

- Akimoto, M., VanSchouwen, B., & Melacini, G. (2018). The structure of the apo cAMP-binding domain of HCN4 – A stepping stone toward understanding the cAMP-dependent modulation of the hyperpolarization-activated cyclic-nucleotide-gated ion channels. *FEBS J*, *285*, 2182–2192.
- Alotaibi, M., Kahlat, K., Nedjadi, T., & Djouhri, L. (2017). Effects of ZD7288, a hyperpolarization-activated cyclic nucleotide-gated (HCN) channel blocker, on term-pregnant rat uterine contractility in vitro. *Theriogenology*, *90*, 141–146.
- Armstrong, W. E., Foehring, R. C., Kirchner, M. K., & Sladek, C. D. (2019). Electrophysiological properties of identified oxytocin and vasopressin neurones. *J Neuroendocrinol*, *31*, e12666.
- Bergman, N. J. (2019). Historical background to maternal-neonate separation and neonatal care. *Birth Defects Res*, *111*, 1081–1086.
- Caldwell, H. K., Aulino, E. A., Freeman, A. R., Miller, T. V., & Witchev, S. K. (2017). Oxytocin and behavior: Lessons from knockout mice. *Dev Neurobiol*, *77*, 190–201.
- Campbell, A. (2010). Oxytocin and human social behavior. *Pers Soc Psychol Rev*, *14*, 281–295.
- Gimpl, G., & Fahrenholz, F. (2001). The oxytocin receptor system: Structure, function, and regulation. *Physiol Rev*, *81*, 629–683.
- Hatton, G. I., & Wang, Y. F. (2008). Neural mechanisms underlying the milk ejection burst and reflex. *Prog Brain Res*, *170*, 155–166.
- Hou, D., Jin, F., Li, J., Lian, J., Liu, M., Liu, X., Xu, Y., Zhang, C., Zhao, C., Jia, S., Jiao, R., Liu, X. Y., Wang, X., Zhang, Y., & Wang, Y.-F. (2016). Model roles of the hypothalamo-neurohypophysial system in neuroscience study. *Biochem Pharmacol (Los Angel)*, *5*, 211.
- Jurek, B., & Neumann, I. D. (2018). The oxytocin receptor: From intracellular signaling to behavior. *Physiol Rev*, *98*, 1805–1908.
- Kalueff, A. V., & Tuohimaa, P. (2004). Grooming analysis algorithm for neurobehavioural stress research. *Brain Res Brain Res Protoc*, *13*, 151–158.
- Li, T., Wang, P., Wang, S. C., & Wang, Y. F. (2016). Approaches mediating oxytocin regulation of the immune system. *Front Immunol*, *7*, 693.

- Lincoln, D. W., Hill, A., & Wakerley, J. B. (1973). The milk-ejection reflex of the rat: An intermittent function not abolished by surgical levels of anaesthesia. *J Endocrinol*, *57*, 459–476.
- Liu, X., Jia, S., Zhang, Y., & Wang, Y.-F. (2016). Pulsatile but not tonic secretion of oxytocin plays the role of anti-pre-cancerous lesions of the mammary glands in rat dams separated from the pups during lactation. *M J Neuro*, *1*, 002.
- Liu, X. Y., Li, D., Li, T., Liu, H., Cui, D., Liu, Y., Jia, S., Wang, X., Jiao, R., Zhu, H., Zhang, F., Qin, D., & Wang, Y. F. (2019). Effects of intranasal oxytocin on pup deprivation-evoked aberrant maternal behavior and hypogalactia in rat dams and the underlying mechanisms. *Front Neurosci*, *13*, 122.
- Lu, T. L., Lu, T. J., & Wu, S. N. (2020). Inhibitory effective perturbations of cilobradine (DK-AH269), a blocker of HCN channels, on the amplitude and gating of both hyperpolarization-activated cation and delayed-rectifier potassium currents. *Int J Mol Sci*, *21*, 2416.
- Morgan, J. I., & Curran, T. (1991). Stimulus-transcription coupling in the nervous system: Involvement of the inducible proto-oncogenes fos and jun. *Annu Rev Neurosci*, *14*, 421–451.
- Neitz, A., Mergia, E., Eysel, U. T., Koesling, D., & Mittmann, T. (2011). Presynaptic nitric oxide/cGMP facilitates glutamate release via hyperpolarization-activated cyclic nucleotide-gated channels in the hippocampus. *Eur J Neurosci*, *33*, 1611–1621.
- Neumann, I., Ludwig, M., Engelmann, M., Pittman, Q. J., & Landgraf, R. (1993). Simultaneous microdialysis in blood and brain: Oxytocin and vasopressin release in response to central and peripheral osmotic stimulation and suckling in the rat. *Neuroendocrinology*, *58*, 637–645.
- Nissen, E., Gustavsson, P., Widstrom, A. M., & Uvnas-Moberg, K. (1998). Oxytocin, prolactin, milk production and their relationship with personality traits in women after vaginal delivery or Cesarean section. *J Psychosom Obstet Gynaecol*, *19*, 49–58.
- Pires da Silva, M., de Almeida Moraes, D. J., Mecawi, A. S., Rodrigues, J. A., & Varanda, W. A. (2016). Nitric oxide modulates HCN channels in magnocellular neurons of the supraoptic nucleus of rats by an S-nitrosylation-dependent mechanism. *J Neurosci*, *36*, 11320–11330.
- Preckel, K., & Kanske, P. (2018). Amygdala and oxytocin functioning as keys to understanding and treating autism: Commentary on an RDoC based approach. *Neurosci Biobehav Rev*, *94*, 45–48.
- Qiu, D. L., Chu, C. P., Tsukino, H., Shirasaka, T., Nakao, H., Kato, K., Kunitake, T., Katoh, T., & Kannan, H. (2005). Neuromedin U receptor-2 mRNA and HCN channels mRNA expression in NMU-sensitive neurons in rat hypothalamic paraventricular nucleus. *Neurosci Lett*, *374*, 69–72.
- Resta, F., Masi, A., Sili, M., Laurino, A., Moroni, F., & Mannaioni, G. (2016). Kynurenic acid and zaprinast induce analgesia by modulating HCN channels through GPR35 activation. *Neuropharmacology*, *108*, 136–143.
- Robichaux, W. G., 3rd, & Cheng, X. (2018). Intracellular cAMP sensor EPAC: Physiology, pathophysiology, and therapeutics development. *Physiol Rev*, *98*, 919–1053.
- Russell, J. A., Douglas, A. J., & Ingram, C. D. (2001). Brain preparations for maternity – Adaptive changes in behavioral and neuroendocrine systems during pregnancy and lactation. An overview. *Prog Brain Res*, *133*, 1–38.
- Sachs, D., Villarreal, C., Cunha, F., Parada, C., & Ferreira, S. (2009). The role of PKA and PKCepsilon pathways in prostaglandin E2-mediated hypernociception. *Br J Pharmacol*, *156*, 826–834.
- Tobin, V. A., Douglas, A. J., Leng, G., & Ludwig, M. (2011). The involvement of voltage-operated calcium channels in somato-dendritic oxytocin release. *PLoS One*, *6*, e25366.
- Uvnas-Moberg, K., & Eriksson, M. (1996). Breastfeeding: Physiological, endocrine and behavioural adaptations caused by oxytocin and local neurogenic activity in the nipple and mammary gland. *Acta Paediatr*, *85*, 525–530.
- van Bodegom, M., Homberg, J. R., & Henckens, M. (2017). Modulation of the hypothalamic-pituitary-adrenal axis by early life stress exposure. *Front Cell Neurosci*, *11*, 87.
- Wakerley, J. B., Clarke, G., & Summerlee, A. J. (1994). Milk ejection and its control. In E. Knobil & J. D. Neill (Eds.), *The physiology of reproduction* (pp. 1131–1177). Raven.
- Wang, P., Wang, S. C., Li, D., Li, T., Yang, H. P., Wang, L., Wang, Y. F., & Parpura, V. (2019). Role of connexin 36 in autoregulation of oxytocin neuronal activity in rat supraoptic nucleus. *ASN Neuro*, *11*, 1759091419843762.
- Wang, S. C., Zhang, F., Zhu, H., Lv, C., Liu, X., Wang, Y.-F., Qin, D., & Currie, S. N. (2016). Suckling-induced burst discharges of supraoptic oxytocin neurons in rats: Prostaglandin mediation of oxytocin actions. *Int J Adv Res*, *4*, 1111–1122.
- Wang, Y. F., & Hatton, G. I. (2005). Burst firing of oxytocin neurons in male rat hypothalamic slices. *Brain Res*, *1032*, 36–43.
- Wang, Y. F., & Hatton, G. I. (2006). Mechanisms underlying oxytocin-induced excitation of supraoptic neurons: Prostaglandin mediation of actin polymerization. *J Neurophysiol*, *95*, 3933–3947.
- Wang, Y.-F., & Hatton, G. I. (2009a). Oxytocin, lactation and postpartum depression. *Front Neurosci*, *3*, 252–253.
- Wang, Y. F., & Hatton, G. I. (2009b). Astrocytic plasticity and patterned oxytocin neuronal activity: Dynamic interactions. *J Neurosci*, *29*, 1743–1754.
- Wang, Y. F., Negoro, H., & Honda, K. (1995). Effects of hemi-transection of the midbrain on milk-ejection burst of oxytocin neurones in lactating rat. *J Endocrinol*, *144*, 463–470.
- Wang, Y. F., Ponzio, T. A., & Hatton, G. I. (2006). Autofeedback effects of progressively rising oxytocin concentrations on supraoptic oxytocin neuronal activity in slices from lactating rats. *Am J Physiol Regul Integr Comp Physiol*, *290*, R1191–R1198.
- Wang, Y. F., Sun, M. Y., Hou, Q., & Parpura, V. (2013). Hyposmolality differentially and spatiotemporally modulates levels of glutamine synthetase and serine racemase in rat supraoptic nucleus. *Glia*, *61*, 529–538.
- Whitley, J., Wouk, K., Bauer, A. E., Grewen, K., Gottfredson, N. C., Meltzer-Brody, S., Propper, C., Mills-Koonce, R., Pearson, B., & Stuebe, A. (2019). Oxytocin during breastfeeding and maternal mood symptoms. *Psychoneuroendocrinology*, *113*, 104581.
- Ying, S. W., Tibbs, G. R., Picollo, A., Abbas, S. Y., Sanford, R. L., Accardi, A., Hofmann, F., Ludwig, A., & Goldstein, P. A. (2011). PIP2-mediated HCN3 channel gating is crucial for rhythmic burst firing in thalamic intergeniculate leaflet neurons. *J Neurosci*, *31*, 10412–10423.